

**EFFECTs OF FINGER WIDTH & FINGER SPACING ON
THE ELECTRICAL PERFORMANCE OF W/CDS BASED
MSM PHOTODETECTOR**

A THESIS SUBMITTED IN PARTIAL FULFILLMENT OF THE
REQUIREMENTS FOR THE DEGREE OF

**MASTER OF TECHNOLOGY
IN
VLSI DESIGN AND EMBEDDED SYStEMS**

By:

**SANTOSH KUMAR PADHY
ROLL NO: 213EC2207**



To the
Department of Electronics and Communication Engineering
National Institute of Technology
Rourkela, Orissa, India
May 2015

**EFFECTs OF FINGER WIDTH & FINGER SPACING ON
THE ELECTRICAL PERFORMANCE OF W/CDS BASED
MSM PHOTODETECTOR**

A THESIS SUBMITTED IN PARTIAL FULFILLMENT OF THE
REQUIREMENTS FOR THE DEGREE OF

**MASTER OF TECHNOLOGY
IN
VLSI DESIGN AND EMBEDDED SYSTEM**

By:

**SANTOSH KUMAR PADHY
ROLL NO: 213EC2207**

**Under the Supervision of
Prof. (Dr.) P.K.Tiwari**



To the
Department of Electronics and Communication Engineering
National Institute of Technology
Rourkela, Orissa, India
May 2015



DEPARTMENT OF ELECTRONICS
AND COMMUNICATION ENGINEERING
NATIONAL INSTITUTE OF TECHNOLOGY, ROURKELA
ODISHA, INDIA-769008

CERTIFICATE

This is to certify that the thesis report entitled “**Effects of Finger Width & Finger Spacing on the Electrical Performance of W/CdS based MSM Photodetector**” submitted by **SANTOSH KUMAR PADHY**, bearing **roll no. 213EC2207** in partial fulfilment of the requirements for the award of **Master of Technology in Electronics and Communication Engineering** with specialization in “**VLSI Design and Embedded Systems**” during session 2013-2015 at National Institute of Technology, Rourkela is an authentic work carried out by him under my supervision and guidance.

To the best of my knowledge, the matter embodied in the thesis has not been submitted to any other university/institute for the award of any Degree or Diploma.

Place: Rourkela

Date: 20th May, 2015

Prof. (Dr.) P. K. TIWARI

Dept. of E.C.E

National Institute of Technology

Rourkela – 769008

Dedicated
To
My beloved Parents

ACKNOWLEDGEMENT

With sincere esteem and deepest gratitude, I would like to express thank my project supervisor **Prof. (Dr.) P.K.Tiwari** who has always been the encouraging force of this project work. His wide-ranging obligation to research work as well as determined strength to gain knowledge and share it with his students had made him a true academician, who has become a source of inspiration for me. I am indebted to him for his valuable guidance, support throughout my project work as well as the good amount of time he had given to me to clarify my doubts and discuss about my work. It has been an honour for me to work with him, and I learned a lot from his superior academic personality.

I express my sincere gratitude to Prof. (Dr) K.K.Mahapatra, Prof. (Dr.) D.P Acharya, Prof. (Dr.) Nurul Islam, Prof.Ayas Kanta Swain, and Prof. Shantanu Sarkar who had introduced the world of VLSI and Embedded System and helped me in grabbing knowledge in various domains of my specialization. I would also like to thank all other faculties and staff of ECE Department, NIT Rourkela for their help and support to complete my project work.

I must express my deep appreciation and gratitude to PhD scholars of Device Simulation Laboratory Mr. Gopi Krishna S, Mr. Visweswara Rao, who were always ready to share their knowledge throughout our course. I also extend my gratitude to my lab-mate Mukesh Kumar Kushwaha, Mukesh Kumar, Ms. Srikanaya for the worthy ideas we had shared on our respective research areas. I am really thankful especially Ashutosh Kumar Singh, Nitin Jain, Naresh Thakur, Anil Rajput, Subhrajit Roy for being my guardian angel and always standing with me during my stay at NIT.I also extend my whole-hearted gratitude to one and all my batch mates and other friends for their immense cooperation without whom my stay in NIT would not have been so enjoyable and memorable.

Last but not least I thank my family whose constant support and encouragement, always help me move forward in life even during hard times.

Finally, I bow myself to Almighty God whose blessings guard and guide me throughout my life.

SANTOSH KUMAR PADHY

ABSTRACT

The metal-semiconductor-metal (MSM) alignment one of the favourable, having the benefit for its simple structure and high detection bandwidths be reach up to gigahertz ranges, constructing them appropriate for very fast on-chip optical connects, and optical communication systems. The detector property parameters like quantum efficiency and response time, stand closely associated to the bounds of electrode geometry plus optical immersion layer, wideness, etc. However, the effect of the device structure on its performance is rarely studied, which limits the development of MSM detectors. MSM structure based Tungsten/Cadmium Sulphide (W/CdS) photodetector (MSM PD) is proposed by using ATLAS Silvaco. The current-voltage (I-V) characteristics of W/CdS photodetector were investigated at different finger widths and finger spacing as well as for different epitaxial layer concentration and thickness of the epitaxial layer. All the simulation has done by illuminating a beam of light of wavelength $8\mu\text{m}$ where peak responsivity we found as 2.96A/W .

Key Words: MSM Photodetector, Finger Width, Finger Spacing

TABLE OF CONTENTS

ACKNOWLEDGEMENTS	iv
TABLE OF CONTENTS	vi
LIST OF FIGURES	ix
LIST OF TABLES	x
1 INTRODUCTION.....	1
1.1 Background.....	2
1.2 Motivation.....	3
1.3 Objective of the Work.....	4
1.4 Thesis Organisation.....	4
2 LITERATURE REVIEW.....	7
2.1 Introduction.....	7
2.2 Background Details.....	7
3 Simulation Methodology.....	13
3.1 Introduction.....	13
3.2 ATLAS Input and Output.....	14
3.3 Direction of Commands in ATLAS.....	15
3.4 Defining Structure using Command Language in ATLAS.....	16
3.4.1 Initial Mesh Specification.....	16
3.4.2 Region and Material Specification.....	17
3.4.3 Electrode Specification.....	17
3.4.4 Doping Specification.....	17
3.5 Outlining Material and Model Parameter.....	18
3.5.1 Contact Characteristics Specification.....	18
3.5.2 Physical Model Specification.....	18

3.6 Optoelectronics Simulator.....	19
3.6.1 Introduction.....	19
3.6.2 Simulating Photodetector.....	19
3.7 Solution Description.....	21
3.7.1 DC Solutions.....	21
3.7.2 Sweeping the biases.....	21
3.7.3 Log Files.....	22
3.7.4 Solve Statements.....	22
3.7.5 Save Statements.....	22
4 METAL-SEMICONDUCTOR INTERFACES-THE SCHOTTKY BARRIER.	24
4.1 Introduction.....	24
4.2 Photodiode Operation.....	25
4.2.1 Schottky Photodiode.....	25
4.2.2 Results and Discussions.....	29
4.3 Summary.....	31
5 PHOTODETECTOR.....	33
5.1 Introduction.....	33
5.2 MSM Photodetector.....	34
5.2.1 Parameter Related to Photodetector.....	35
5.3 Advantages of MSM Photodetector.....	37
5.4 Summary.....	38
6 PROPOSED MSM PHOTODETECTOR.....	40
6.1 Introduction.....	40
6.2 Proposed MSM Structure.....	40
6.3 Results and Discussions.....	42

7	CONCLUSION.....	49
	7.1 Outcome of the Work.....	49
	7.2 Future Scope.....	49
	REFERENCES.....	50

List of Figures

Fig.1 Input and Output Flow of ATLAS.	13
Fig.2 Band diagram for metal-semiconductor junction at zero bias (equilibrium) showing Schottky barrier height, Φ_B , for an n -type semiconductor as the difference between the interfacial conduction band edge E_C and Fermi level E_F	24
Fig.3 ATLAS Structure of a Schottky diode under dark condition.	26
Fig.4 ATLAS Structure under illumination of light of wave length 8 μm	27
Fig. 5 Dark and Photo I-V Characteristics at different bias voltages.	27
Fig.6 Classification of Photodetector.	29
Fig.7 Schematic of MSM detector.	31
Fig.8 Schematic of Proposed MSM Photodetector.	36
Fig.9 Energy band diagram of MSM Photodetector.	36
Fig.10 Proposed Structure under dark condition.	37
Fig.11 Structure of MSM photodetector under illumination of light of wavelength 8 μm	37
Fig.12 Responsivity at various wavelength.	38
Fig.13 Dark current-voltage characteristics of proposed MSM with different finger widths for finger spacing (a)2 μm (b) 5 μm	39
Fig.14 Illuminated current-voltage characteristics of proposed MSM per different finger widths at finger spacing (a)2 μm (b) 5 μm	39

Fig.15 Dark current-voltage characteristics of proposed MSM with changed finger spacings at finger width (a)2 μm (b) 5 μm	40
Fig.16 Photo current-voltage characteristics of proposed MSM Photo-detector with altered spacing.	41
Fig.17 Current-voltage characteristics of proposed with changed epitaxial carrier concentration.(a)Dark I-V characteristics (b) Illuminated I-V characteristics. ...	41
Fig.18 Dark current-voltage characteristics of proposed photo-detector per epitaxial layer widths. (a) $N_d=1 \times 10^{15}/\text{cm}^3$ (b) $N_d=5 \times 10^{16}/\text{cm}^3$	42
Fig.19 Photo current-voltage characteristics of proposed per epitaxial layer widths. (a) $N_d=1 \times 10^{15}/\text{cm}^3$ (b) $N_d=5 \times 10^{16}/\text{cm}^3$	42

List of Tables

Table 1 Order of ATLAS Commands.	13
Table 2 Syntax for Initial Mesh Specification.	14
Table 3 Syntax for Specifying Region and Material.	15
Table 4 Syntax for Specifying Electrode.	15
Table 5 Syntax for Doping Specification.	15

Introduction

Background

Motivation

Objective of the Work

Thesis Organisation

1. Introduction

1.1 Background

In recent times, we have seen a robust demand of IR technology and is now thinkable to apply it in remote sensing application. Several materials scrutinized in the IR field emphasized predominantly on longer wavelengths of 3-5 μm and 8-14 μm for their use in communication applications [1]. The metal-semiconductor-metal (MSM) alignment one of the favourable, having the benefit for its simple structure and high detection bandwidths be reach up to gigahertz ranges, constructing them appropriate for very fast on-chip optical connects [2], and optical communication systems [3].

In disparity to a p–n junction as per in a photodiode, a MSM photodetector is a device that comprehending two Schottky contacts back to back. In the course of action, some electric voltage is delivered to the electrodes and as soon as light encroaches on the semiconductor among the electrodes, which causes electron-hole duos and these electric carriers were swept by the electric field and giving rise photocurrent to flow across the device. To boost the performance of photodetector, metallic electrodes with dissimilar types and sizes were embedded in designing the photodetectors [4–6]. The set-up of inter-digital metallic electrodes in MSM photodetectors commanded to an effectual light absorption as well downscaling the device active region [7]. Additionally, the electrical possessions of the photodetector can be upgraded by growing the photocurrent, accomplished by improving the rates of photo-generated carriers [8], and dropping the dark current caused due to the Schottky barriers sandwiched between the metal and the semiconductor boundary [9,10]. MSM detectors have high demand for its low intrinsic capacitance and high responsivity.

Cadmium Sulphide (CdS) belonging to the II-VI direct bandgap compound semiconductor group is widely known as an n-type window material for optoelectronic devices [11-14]. CdS is a wide bandgap semiconductor material ($E_g = 2.4$ eV) with having ultrafast response and good stability for visible-light detectors. As for photo detection CdS is integrating with a different inferior bandgap semiconductor in suitable arrangement of energy levels, broaden the response spectra to longer wavelength forthcoming headed for adjacent to infrared range. On the other hand, the low responsivity continually restricts their real-world application. Therefore, finding an operational way to heighten the photo current of CdS based detectors come to be significant. The detector property parameters like quantum efficiency and response time, stand closely associated to the bounds of electrode geometry plus optical immersion layer, wideness, etc. However, the effect of the device structure on its performance is rarely studied, which limits the development of MSM detectors.

1.2 Motivation

A photodetector is a device that transforms the light energy hooked on to some other custom of energy, such as thermal or electrical energy. An accumulative amount of consideration is being waged to assimilating high-speed photodetectors with microelectronic and photonic circuits. Integration with electrical circuits amplifies the enactment by eradicating the parasitic and restricted bandwidth of bonding pads, wires, and connectors. Integration by means of optical waveguides declines the optical damage related with connection from one device to another and diminishes the wrapping cost. The modern applications of photodetectors are numerous and they are important for fibre optics. The metal-semiconductor-metal (MSM) alignment one of the favourable, having the benefit for its simple structure and these detectors can be made

quicker than photodiodes. Their exposure bandwidths can spread hundreds of gigahertz, building them appropriate for very fast optical fibre communications.

1.3 Objective of the work

In this thesis, a W/CdS MSM photodetector is proposed using two-dimensional device simulators using ATLAS Silvaco. ATLAS is a physically-based two and three dimensional device simulator that is used to estimate the electrical playacting of semiconductor devices at quantified bias environments. It resolves the important physical calculations relating the dynamics of carriers in semiconductor devices for random device arrangements. It forecasts terminal individualities of semiconductor devices aimed at steady state, transient, and small signal AC incitements .It gives vision into the interior appearances of semiconductor devices [15]. The detector property parameters like quantum efficiency and response time, stand closely associated to the bounds of electrode geometry plus optical immersion layer, wideness, etc. However, the effect of the device structure on its performance is rarely studied, which limits the development of MSM detectors. The effect of finger width, finger spacing on current at different biases on current-voltage characteristics of photodetector have studied. The impact of epitaxial layer concentration and thickness of the epitaxial layer on existing has also been considered for optimum device structure.

1.4 Thesis Organization

This thesis is prearranged into six subdivisions. The present chapter begins with the contextual details of MSM photo detector. The objective for this thesis work is framed and ends with the outline of the thesis.

Chapter-2

This chapter discourses the literature review in more details which deals various types of MSM photodetector.

Chapter-3

This chapter discusses about simulator methodology i.e. Optoelectronics simulator we used for the simulation of MSM photodetector in more detailed way.

Chapter-4

This chapter discusses about the schottky diode followed by structure of the proposed schottky diode and the current-voltage characteristics of the proposed.

Chapter-5

The purpose of this Chapter is to present the structure of a basics of MSM photo detector and the advantages over schottky diode. It also discusses about the important parameter related to the photo detector.

Chapter-6

This chapter presents the proposed MSM photodetector and the current-voltage characteristics is carried out by varying different geometrical parameter like finger width, finger spacing, thickness and concentration of epitaxial layer.

Chapter-7

The last chapter is a summary and discussion on the work presented in this thesis where also further work is outlined.

Literature Review

Introduction

Background details

2. Literature review

2.1 Introduction

Recently, MSM photo-detector have developed progressively common in the exploration ground due to their key benefits like:

- Modest structure.
- Simplicity of fabrication also assimilation.
- Short capacitance per unit area.

MSM detectors are comprise of two end-to-end schottky diodes by way of an inter-digitized electrode arrangement on higher of a lively light assembly region. This photodetector cannot work absence of any biasing [16]. These photodiodes are naturally having high speed due to their short capacitance for each unit area and are commonly passage time limited, not time constant limited. Using proper fabrication steps, the electrode spacing and width can be set to micron length causes to enhance the speediness significantly. The principal downside of MSM detectors is their expected small responsivity. MSM devices show stumpy photo-responsivity principally due to their metallization of the electrodes shades at the lively light gathering section.

2.2 Background Details

In recent times, II–VI semiconductors has been seen a speedy development in the field of designed due to their usage in solar chambers. Cadmium sulphide (CdS) belonging to this group is the utmost broadly used material for CdS/CdTe and CdS/Cu₂S heterojunction solar cells due to the presence of intermediary energy band gap with reasonable transformation efficiency, steadiness and near to the ground cost. D. Patidar

et al in their review provides a comprehensive overview of the progress made in the growth of Cadmium sulphide (CdS) which can be very useful for optoelectronic, piezo-electronic and semiconducting material [17].

Munir et al. in this paper investigated on finding the optimal room temperature current-voltage physical characteristics on an n type GaN schottky diode by using different contacts of many sole layer metal (Pt, Ni, Au, Ti, Al, Sc). The simulated current was obtained by increasing forward bias from 0~ 4Volt accompanied by using Atlas/Blaze advanced by Silvaco. Different models like incomplete ioniz, Bgn, cvt, Fermi, Shockley- Read Hall was used to get optimal current-voltage characteristics. It was found that metals Pt, Ni, Au exhibit strong rectifying behaviour while Al and Ti exhibit weak rectifying properties. It has also been found out that with the enhance in the metal work function that is correlated with a growth trendy the barrier height. By manipulating the values of barrier height (Φ_B), breakdown voltage (VB), ideality factor (η) for the different electrodes, they came to a conclusion that Platinum (Pt) metal display the optimal (I-V) rectifying characteristics with n-GaN schottky diode [18].

Weng et al. in this paper investigated for an n-CdS/p-PbSe heterojunction. A tinny CdS film is placed by chemical bath deposition on upper of the epitaxial PbSe film by molecular beam epitaxy on Silicon. Current-voltage measurements demonstrate very good junction characteristics with rectifying ratio of 178 and Ideality factor of 1.79 at 300 K. Detectors made with such structure shows mid-infrared spectral photo response at room temperature [19].

Ito et al. here presented a metal-semiconductor-metal photodiode consist of a semiconductor layer and two electrode cathode and anode which are designed on the semiconductor deposit and are made of such commonly different electrode resources that the cathode electrode has a Schottky barrier height Φ_{bn} from a conduction band satiating $\Phi_{bn} > E_g/2$ and the anode electrode has a Schottky barrier height Φ_{bp} , from a valence band filling $\Phi_{bp} > E_g/2$, where E_g symbolises the energy band gap. The existing invention uses dissimilar electrode resources for the anode and the cathode electrodes separately for the MSM photodiode so as to shrink the dark current further [20].

Berger et al here disclosed an improved metal-semiconductor-metal (MSM) photodiode, specifically a new high responsivity and high bandwidth photodetector, resulting in a high gain-bandwidth product which is an MSM photodiode in which the anode and cathode are made of different materials of differing opacity and possibly including different electrode dimensions as well. Using an opaque anode and a transparent cathode reduces surface reflections off the opaque electrodes allowing more light to be absorbed within the active semiconductor region. However, it concurrently keeps the transit distance for the slower moving holes to a minimum. Thus, the long tail in the impulse response due to hole collection is minimized, resulting in increased bandwidth [21].

An et al. here fabricated and characterised a MSM photodetectors established on graphene/p-type Silicone Schottky junctions. Here Thermionic emission controls the current transport controls through the mainly caused due to Thermionic emission through the junctions above 260K in absence of biasing of 0.48 eV barrier height. In reverse biasing the necessity of the barrier height is initiate to outcome typically

commencing the Fermi level to move in graphene. MSM detectors unveil a responsivity of 0.11A/W and a standardised ratio of photocurrent-to-dark current is found $4.55 \times 10^4 \text{mW}^{-1}$, that are superior to those previously achieved for comparable detectors grounded on carbon nanotubes. The finding are significant for assembling the translucent, conducive graphene electrodes hooked on prevailing silicon expertise [22].

WANG et al here fabricated a GaN MSM UV detectors with titanium tungsten (TiW) as translucent electrodes and current- voltage characteristics also considered. This finding shows the TiW film of 10-nm-thick dropped with RF power of 300 W can still deliver a sensibly high transmission at 300 nm 75.1%, a low resistivity of $1.7 \times 10^3 \text{ cm}$ and an effective 0.773 eV of Schottky barrier height on the proposed MSM. They as well reached an uttermost 0.192 A/W of responsivity and a 66.4% of quantum efficiency from the presented GaN UV MSM detector as TiW electrodes. Under the application external biasing of 3V, it was shows smallest noise equivalent power of $1.987 \times 10^{-10} \text{ W}$ [23].

Zhang et al. here simulated a 4H-SiC MSM UV photodetector and the current-voltage (I-V) characteristics has been found out with different finger widths and spacing, different carrier concentrations and thicknesses of N-type epitaxial layer. The simulation outcomes signpost that both the dark current and the photocurrent rise when the finger width upsurges. But the consequence of finger width on the dark current is more noteworthy. While the other hand, the outcome of finger spacing on the photocurrent is weightier. It has been found out that with the increase in finger spacing, the photocurrent falls and the dark current is almost unalterable. In accumulation, it is found that the lesser the carrier concentration of n-type epitaxial layer is, the less

significant the dark current and the superior the photocurrent will be. It is also found that the current of MSM photodetector also rest on the epitaxial layer thickness [24].

Chen Bin et al. presented a model of a 6H-SiC MSM UV photodetector based on thermionic emission theory is recognised with the simulation set of ISE-TCAD. The current-voltage characteristics of the device has been found out for 3 μm finger width (W) and electrode spacing (L) of 3 μm . The findings expresses that the proposed at 10 V bias shows fairly a little dark current of 15 pA and the illuminated current is double to that of dark current. The effects of finger width and spacing on dark and photo I-V characteristics of the MSM detector are examined to enhance the device constraints [25].

Simulation Methodology

Introduction

ATLAS Input and Output

Direction of Commands in ATLAS

Defining Structure using Command Language in ATLAS

Outlining Material and Model Parameter

Optoelectronic Simulator

Solution Description

3. Simulation Methodology

3.1 Introduction

ATLAS is physically built device simulator which provides platform to the device engineers to study and characterised the behaviour of semiconductor devices. It enables the researcher to simulate the optical, thermal and electrical behaviour of the device. ATLAS gives a platform for a physical centred, flexible, stress-free to put into practise and extensible stage to realize DC, AC and time field reactions for semiconductor device technologies in 2D and 3D. As a result it relates simulation very carefully to technology improvement and ensuing in the expressively increased assistances from simulation practice [15].

ATLAS devises a prefabricated design that consist of the ensuing licensable outfits and additions:

- ❖ **ATLAS:** Delivers universal abilities that are retrieved by totally the device simulation produces.
- ❖ **S-PISCES:** Uses for simulation of silicon devices.
- ❖ **LUMINOUS:** Supplies skills required to act out optoelectronic devices
- ❖ **LASER:** Used for heterostructure lasers with explanation of the Helmholtz equation aimed at photosensitive field.
- ❖ **MIXEDMODE:** That deal with numerical physically-based devices as well as compacted logical models with competences to circuit simulation.

ATLAS, a simulator used to simulate physical devices that calculates the electrical features which are related with quantified physical arrangement and bias settings. To realise this, we need to approach the action of a device against 2D or 3D grid comprising

number of grid points called as nodes. Through considering the certain differential equalities, resulted from Maxwell's laws and applying it to this grid points, the carriers transport through the structure is now imaginable. This indicates that AC, DC, or transient modes of procedure can be demonstrated on electrical performance of the device.

Application to this type simulation has become very significant for two cause. Primarily, it is ample faster and inexpensive than acting experiments. Secondly, it affords data that is either hard or terrible to extent. The disadvantage of this simulation are altogether related physics need to be combined into the simulator, and mathematical techniques must be followed to resolve the related equalities. These jobs have to be handled by the users of ATLAS. ATLAS user must specify the problem of device simulation by describing:

- ❖ The physical device which is going to be simulated
- ❖ The model which we need to include
- ❖ Biasing conditions for the electrical characterisation

3.2 Atlas Input and Output

The movement of excitation and response for the ATLAS as shown in figure3. Most ATLAS simulation have two excitation files i.e. text file which contains commands to ATLAS for execution and second contains the structure folder which states the structure that we want to simulate. ATLAS creates three kinds of output files, i.e. the current and voltage characteristics from device scrutiny. Third sort of this i.e. which stores 2D and 3D data involving to the principles of solution variables inside the device at a certain bias point [15].

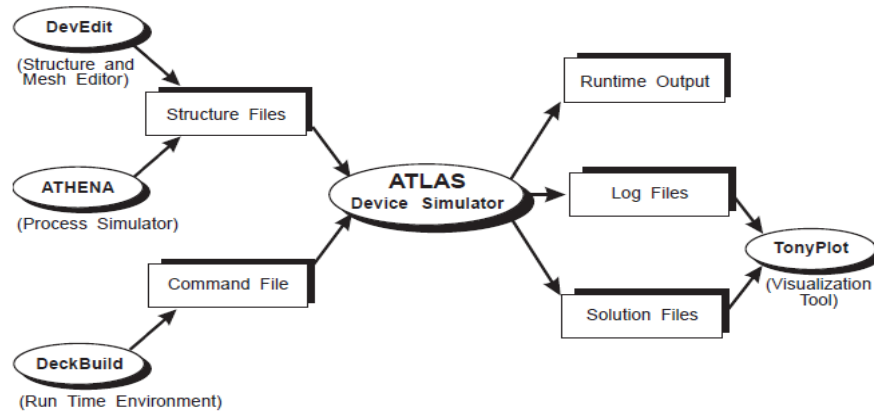


Fig.1 Input and Output Flow of ATLAS

3.3 Direction of Commands in ATLAS

The statement order which is going to occur in input file in ATLAS is vital. We have five groups in ATLAS that should occur in correct order which as shown below. Any deviation leads to error causes to improper operation or cessation of the program.

Serial No.	Group	Statements
1.	Structure Specification	MESH REGION ELECTRODE DOPING
2.	Material Model Specification	MATERIAL MODELS CONTACT INTERFACE
3.	Numerical Method Selection	METHOD
4.	Solution Specification	LOG SOLVE LOAD SAVE
5.	Result Analysis	EXTRACT TONYPLOT

Table 1 Order of ATLAS Commands.

Correct order in defining mesh, structure, and specifying the solution should be strictly followed. Any deviation leads to error causes to improper operation or cessation of the program [15].

3.4 Defining a Structure using Command Language in ATLAS

At first we need to define mesh while defining a structure in ATLAS. This mesh can be explained as a sequence of horizontal and vertical streaks and spaces between these lines. Regions inside this mesh are assigned to dissimilar materials according in the direction of our requirement intended for constructing proposed device. After defining regions next step is to specify the electrode and at last the doping of each region is need to be specify.

3.4.1 Initial Mesh Specification

Initially we need to define the Mesh which can be written using the command language as:

This statement come first before x.mesh and y.mesh statement.

Statement	Comment
Mesh space.mult=<value>	Spac.mult factor cast-off as a factor aimed at the obtained mesh by the declarations x.mesh and y.mesh. This will be one for default case and lesser value will create finer mesh.
x.mesh location=<value> spacing=<value> y.mesh location=<value> spacing=<value>	This two statements used to state the positions in microns of vertical and horizontal streaks along by way of spacing associated to each line. It should be state with the increase order of x and negative value also allowed

Table 2 Syntax for Initial Mesh Specification.

3.4.2 Region and Material Specification

After defining the mesh next step is to define each part with a material type which is done through REGION statements as follows:

REGION num=<integer> / <material type> <position parameters>	Region number should begin with one and increases for each succeeding region. The position constraints are defined by using x.minimum,x.maximum,y.minium,y.maxmium in microns.
---	--

Table 3 Syntax for Specifying Region and Material.

3.4.3 Electrode Specification

Once specifying the region and material we need to define electrode that works as a contact for the semiconductor using the command as follows:

Statement	Comment
ELECTRODE NAME=<electrode name><position parameter>	The position parameters are described by using x.max, x.min, y.max, y.min in microns.Upto 50 electrode can be specified with same name also.

Table 4 Syntax for Specifying Electrode.

3.4.4 Doping Specification

DOPING <distribution type><dopant type><position parameters>	Doping profile can either be Gaussian or uniform.
--	---

Table 5 Syntax for Doping Specification.

For example:

```
DOPING CONCENTRATION=1E18 P.TYPE GAUSSIAN CHARACTERISTIC=0.5  
X.LEFT=1.0 X.RIGHT=2.0 PEAK=0.1
```

This declaration specifies a p-kind of Gaussian profile by means of a peak concentration of $10^{18}/\text{cm}^3$ topmost doping positioned sideways a line on or after $x=1$ to $x=2$ microns.

3.5 Outlining Material and Model Parameter

After defining the mesh and geometry, we need to change the properties of electrodes in the next step where we also need to choose the model for our device simulation which can be done as described below:

3.5.1 Contact characteristics specification

To define an electrode as Schottky we need to mention the work function of the metal otherwise it will be treated as an Ohmic contact. The NAME factor is used for denoting which electrode and its characteristics have to be modified.

For example:

```
CONTACT NAME=ANODE WORK FUNCTION=4.55
```

This statement indicates that here anode we used as metal of work function 4.55 eV which represents the work function of Tungsten (W).

3.5.2 Physical Model Specification

The physical model is divided into five classes as mobility, impact ionization, recombination, tunnelling and carrier statistics. All models can be specified using the MODEL statement while impact ionization is specified by using IMPACT statement.

For example:

```
MODELS ANALYTIC AUGER FLDMOB IONIZ
```

Syntax specifies Concentration and Temperature Dependent mobility, AUGER recombination, parallel field mobility, and Silicon Ionization Model statistics.

3.6 Optoelectronic Simulator

3.6.1 Introduction

Luminous is a wide-ranging tenacity light circulation and absorption program combined into ATLAS framework. It used to calculate the optical intensity profiles inside semiconductor device. The intensity files then converted into photo generation rates, which are directly into the generation terms in the carrier continuity equations. These tools allows us to simulate the electrical reactions to photosensitive signals for a wide range of photosensitive detector which consist of photodiodes, Schottky photodetectors, avalanche photodiodes, solar cells, and MSM photodetector [15].

3.6.2 Simulating Photodetectors

This sections explains the technique is used for simulation of photodetectors which can be applied to avalanche photodiodes, CCDs, Schottky photodiodes, MSMs and other optical triggered devices.

Defining Optical Sources

Recognising an Optical Beam:

Photosensitive sources can be described by using BEAM statement which must be mentioned anywhere next to MESH, REGION, DOPING, and ELECTRODE statements and before SOLVE statement. Maximum ten optical sources can be defined. The NUM parameter used for unique identifying one photosensitive source whose value can be varies from 1 to 10. B<n> parameter is used to set the power of the optical beam, everyplace n represents the beam digit demarcated by NUM.

Beam Origin Plane for Optical Sources:

Optical source origin can be used by using X.ORIGIN and Y.ORIGIN parameters which define the source of the optical beam qualified to the device coordinate structure. At present it should lie outside the device region. The direction of beam propagation

with respect to the device coordinate system can be specified by using ANGLE parameter. ANGLE=90 shows vertical illumination from above. MAX.WINDOW and MIN.WINDOW parameter is used to specify the width of the optical beam.

Obtaining Quantum Efficiency versus Bias

The intensities mentioned in the SOLVE declaration till another SOLVE statement modifies the intensity of the beam. Simple optical intensity of linear ramps can be specified using the NSTEP and LIT.STEP parameters in solve statement Where NSTEP describes the number of steps and LIT.STEP represents the size of the DC step.

Finding Transient Reaction of Optical Bases

It is at times required to find out the time dominion output of the optoelectronic device to know the time dependant of the optical sources. RAMP.LIT parameter specified in LUMINOUS must be mentioned in a SOLVE declaration where the optical power will change from the utmost lately set strength to the given power mentioned in B parameter. The RAMPTIME parameter will specify the linear ramp period and TSTOP parameter specifies where the transient simulation will stop. TSTEP also should be set for transient response which allows several samples within the RAMPTIME. Sample example shown below gives the specification for an optical source [15].

For example:

```
SOLVE B1 RAMPTIME=10E-9 TSTOP=30E-9 TSTEP=1E-11
```

Obtaining the Spectral Response

The device current as a function of wavelength called as spectral response can be found. The LAMBDA factor in SOLVE statement use to fix the wavelength of the beam in microns. We should specify the initial and final wavelength and the step size of the wavelength as mentioned below:

SOLVE BEAM=1 LAMBDA=0.2 WSTEP=0.1 WFINAL=0.8

Here the spectral response is obtained for initial wave length given 0.2 microns till 0.8 microns (WFINAL) with a step size of 0.1 microns.

3.6.2.5 Obtaining Angular Response

The output of detector also can be find out with respect to angle of incidence by using the following:

SOLVE BEAM=1 ANGLE=0.0 ASTEP=10.0 AFIANL=60.0

This allows collection of response versus angle. Here we get angular response from 0 degree to 60 degree with a step of 10 degree.

3.7 Solution Description

ATLAS is used to find AC, DC and transient explanations. Mostly voltage are specified aimed at each electrodes. It calculates current for each node.

3.7.1 DC Solutions

SOLVE statement is meant for mentioning the voltage for each node.

For example:

SOLVE VANODE=0.1 # statement resolves a sole bias point per 0.1 V on electrode named anode.

3.7.2 Sweeping the bias

A sweep bias may be required which can be specify given syntax.

SOLVE VANODE=0.1

SOLVE VCATHODE=1.0 VSTEP=1.0 VFINAL=20.0 NAME=CATHODE

The above statement describes to show the variation in Cathode voltage from 1V to 20V at step 1V with fixed anode voltage=0.1V

3.7.3 Log Files

This is used to keep the terminal characteristics that are manipulated by ATLAS which may be current or voltage for each and every electrode in DC simulations.

LOG OUTF=<FILE NAME.log>

This file contains the terminal characteristics which can be viewed in TONYPLOT.

3.7.4 Solve Statement

This used to generate SOLVE statements which is a worksheet style record.

3.7.5 Save Statement

The OUTFILE parameter is used either with the SOLVE or SAVE statements, to generate a structure file.

Syntax: SAVE OUTF=<file name.str>

Metal-Semiconductor Interfaces-The Schottky Barrier

Introduction

Photodiode Operation

Summary

4. Metal-Semiconductor interfaces

- The Schottky Barrier

4.1 Introduction

Schottky barriers are a vital component for numerous semiconductor devices, including MSM photodetectors. For MSM photodetectors, it is essential that the metal contacts exhibit a good rectifying characteristics, over the functional range of bias voltage. This safeguards low dark current and minimal inferior carrier injection which affects the noise and speed appearances of the MSM detector.

In any incident a perfectly well-ordered and intimate metal-semiconductor contact is a theoretical concept. Metals placed on semiconductors habitually are polycrystalline and the electronic specifics at the interface are reliant on the precise structure. In addition even for metal deposited in high vacuum the surface always becomes disordered as metal atoms diffuse into the semiconductor and vice-versa. Also new phases are formed due to chemical reactions between the metal and semiconductor atoms.

This chapter gives a brief enlightenment to the basic operation principles of Schottky diode and the design fundamentals for optical simulations. A metal–semiconductor–metal photodetector (MSM detector) is a detector encompassing two Schottky contacts, i.e., two metallic electrodes arranged on a semiconductor material, in difference to a p–n junction as in a photodiodes. When a metal comes closer contact with a semiconductor material forms an M–S junction that can both be non-rectifying or rectifying. The rectifying metal-semiconductor junction offers rise to a Schottky barrier, known as a Schottky diode, while the non-rectifying one is called as an ohmic

contact. (In dissimilarity, to a semiconductor–semiconductor joint a rectifying and the mostly commonly used semiconductor device at present, is known as a p–n junction.) We will first explain the theoretical background for a Schottky diode. Functioning principles of Schottky diode discoursed in the subsequent sections [26].

4.2 Photo diode operation

When light incident on a junction of a photodiode, photons having energy superior than or equal to bandgap energy of the semiconductor are engrossed and superfluous electron-hole pairs are produced and then detached via the recognised field in the depletion region. Once the photodiode is connected over an external load in a circuit, a quantifiable current flows through the circuit which is comparative to the number of photons absorbed and the photo-generated carriers.

4.2.1 Schottky photodiodes

A Schottky barrier, is a potential energy blockade for electrons shaped at a metal–semiconductor joint, named after Walter H. Schottky. Schottky barriers having the rectifying features, appropriate for practise by way of a diode. Some of the principal appearances of a Schottky barrier is the Schottky barrier height, denoted by Φ_B as shown below figure. The importance of Φ_B depend on the arrangement of semiconductor and metal. All M-S junctions does not produce a rectifying Schottky barrier; a M-S junction that allows the current flow in both directions lacking rectification, possibly due to its Schottky barrier presence being too little, is known to be an ohmic contact.

A non-rectifying ohmic contact: is the electrical junction which follows with Ohm's law formed among two conductors showing a linear current–voltage curve. The application of low-slung resistance ohmic contact is to permit charge to flow simply in

both sides between the dualistic conductors, deprived of stalling due to modification or surplus power indulgence due to voltage onsets. Distinction to this, a junction that which does not follow a linear current–voltage curve is termed to be non-ohmic which emanate several of forms (rectifying heterojunction, p–n junction, breakdown junction, Schottky barrier etc.). Usually the term "ohmic contact" obliquely signifies a metal contact near to a semiconductor, where attaining ohmic behaviour is thinkable but needs watchful procedure. While the metal–metal ohmic connections are somewhat easier to fabricate, by verifying straight connection between the metals without intervening coats of insulating dirtiness or oxidation; several methods are used to generate ohmic metal-metal junctions (soldering, crimping, welding, electroplating, deposition, etc.). This text emphasises on M-S ohmic contacts. Both Schottky barriers and ohmic contacts which predominantly reliant on the Schottky barrier height, which sets the threshold for the additional energy an electron entails to permit originating to the metal from the semiconductor. Intended to the junction to acknowledge electrons effortlessly in mutual directions (ohmic contact), the barrier height must be minor in at minimum around parts of the connection surface. To provide an admirable ohmic connection (low resistance), we need to keep the barrier height as minor as possible and additionally it must not redirect electrons at the boundary. The Schottky barrier height among a metal and semiconductor which is ingenuously projected by the Schottky-Mott rule are reliant on to the alteration of the metal-vacuum work function and the electron affinity of vacuum- semiconductor. In preparation, maximum metal-semiconductor boundaries do not monitor this instruction to the anticipated degree. Instead, the chemical closure of the semiconductor crystal beside a metal generates electron states inside its band gap. Thus the elevations of the Schottky barriers in metal-semiconductor connections frequently display little

dependency on the value of work functions of semiconductor or metal, in unambiguous difference to Schottky-Mott rule. Unlike semiconductors display this Fermi level pinning to dissimilar degrees, but a technical significance is that high quality (low resistance) ohmic contacts are habitually challenging to form in significant semiconductors such as arsenide and silicon. The Schottky photodiode is based around the Schottky barrier diode that may also be called the metal-semiconductor diode due to its structure [26].

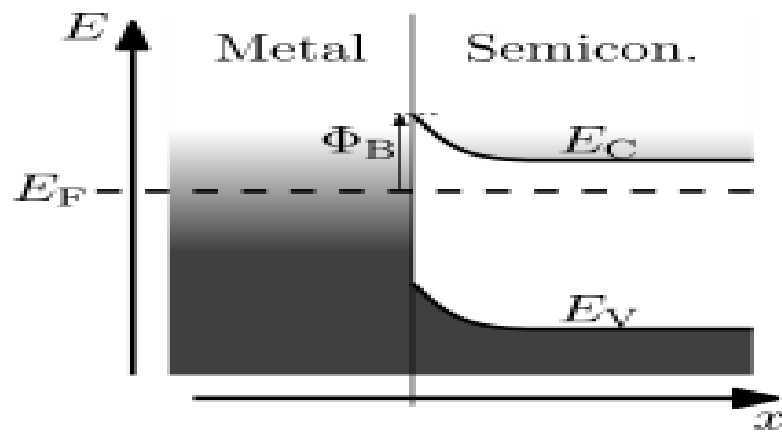


Fig.2 Band diagram for metal-semiconductor junction at zero bias (equilibrium) showing Schottky barrier height, Φ_B , for an *n*-type semiconductor as the difference between the interfacial conduction band edge E_C and Fermi level E_F .

In difference to a p-n diode, the current transport mechanism for a metal-semiconductor contacts is largely caused due to majority carriers. There are principally four dissimilar transport mechanisms: thermionic emission over the barrier, carrier recombination or generation in the depletion region, tunnelling through the barrier, and in the neutral region of the semiconductor due to carrier recombination. Thermionic emission is the governing transport mechanism, which creates the perfect diode characteristics. Thermionic emission concept is imitative by Bethe aimed at high-mobility semiconductors, and diffusion concept is derived by Schottky intended for low-

mobility semiconductors. Finally, a mixture of the two methodologies has been projected by Crowell and Sze. The expression for the current density-voltage characteristics of a schottky diode is given by the following equations.

$$J=J_s (e^{qV/KT}-1)$$

$$J_s=A^{**}T^2 \exp (-qB/KT)$$

Schottky photodiodes the fastest of photodiodes available that can be used for sensing UV and visible radiation. However the disadvantage of having low quantum efficiency caused due to thin absorption regions and the highly absorbing schottky metal. Supplying adequately high reverse bias voltages, the entire N- region (active region) can be depleted, ensuing in a continuous electric field across the region. Photons with energies larger than the band gap are absorbed in the depletion area and electron-hole couples are engendered. The electric field remove the generated electron- hole duos. Electrons drift to the N+ doped semiconductor, holes drift to Schottky metal and an output current develops in the external circuit [26].

The Schottky photodiode having the additional benefits over other forms of photodiode in terms of speed and long wavelength detection capability. As a result the Schottky photodiode has a unique position in amongst the other forms of photodiode that are available. The Schottky photodiode is a diode with forward voltage drop very low having very fast transferring action. An M-S junction is made sandwiched in the middle of a semiconductor and a metal, generating a Schottky barrier (as an alternative of a semiconductor–semiconductor join as in orthodox diodes). Distinctive metals used are platinum, molybdenum, certain silicide e.g. palladium silicide and platinum silicide, and tungsten or chromium; and the semiconductor classically be n-type. Metal on one

side acts as anode and n-type semiconductor performs as the cathode of the diode. This Schottky barrier outcomes trendy cooperation very dissolute transferring and low frontward voltage drip.

4.2.2 Results and Discussion

Figure 3 shows the structure of proposed MS photo diode fabricated on a 0.5 μm thick n-type CdS epitaxial layer, with a doping concentration of $3 \times 10^{15} \text{ cm}^{-3}$, which grows on a 1 μm thick, $5 \times 10^{18} \text{ cm}^{-3}$ doped n^+ CdS substrate under dark conditions. Schottky contacts on the epitaxial layer are formed by defining a 200-nm-thick gold (Au) interdigitated contact electrode. Figure 4 shows under illumination of light of wave length 8 μm .

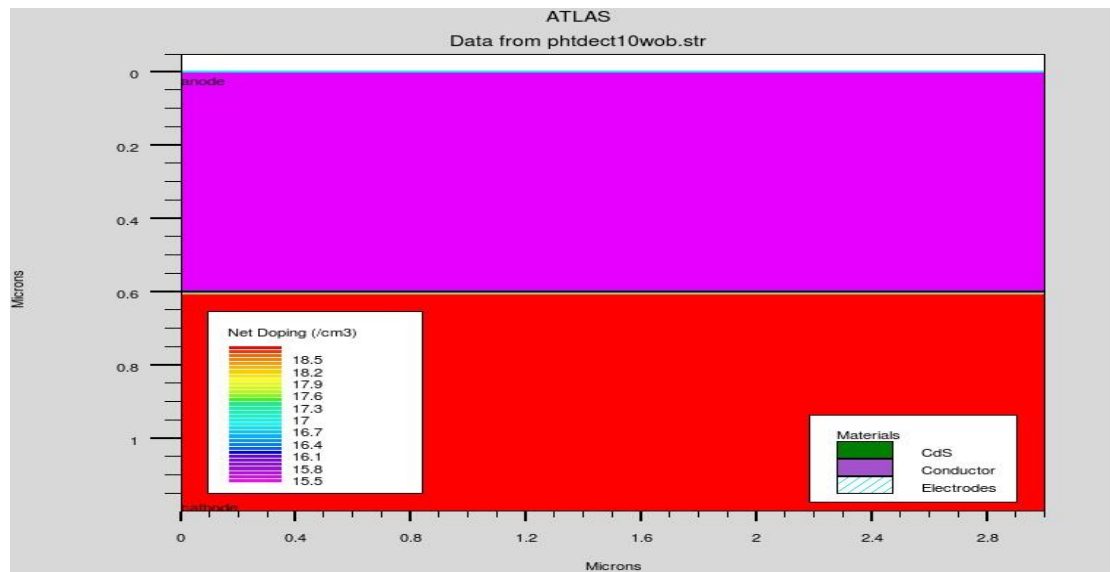


Fig.3 ATLAS Structure of a Schottky diode under dark condition.

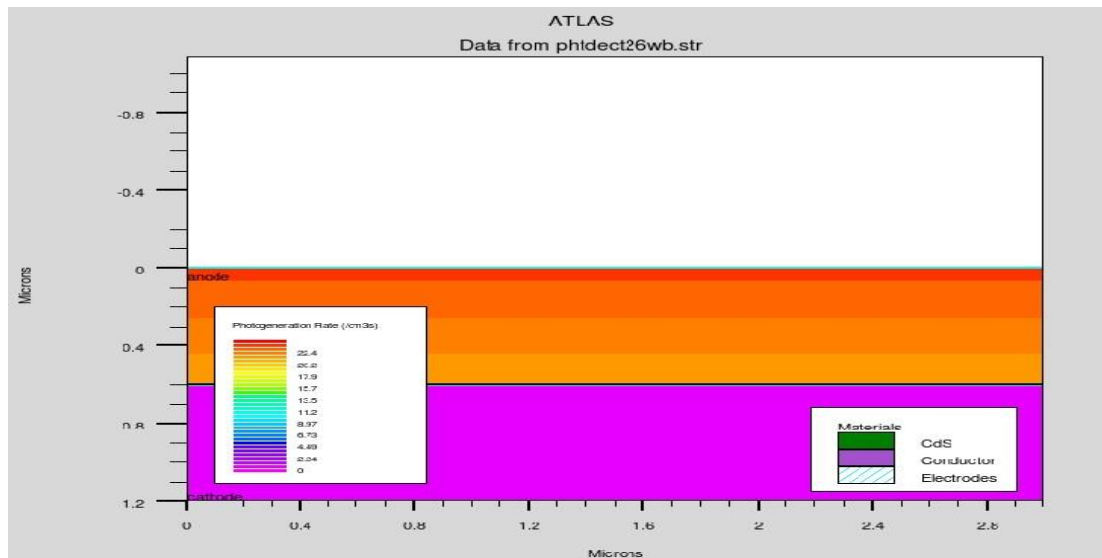


Fig.4 ATLAS Structure under illumination of light of wave length 8 μm .

The dark current and photo current was found out under different bias voltages. Photo current (green line) was found more as compared to dark current (red line).The graph between I-V as shown below (fig.5).

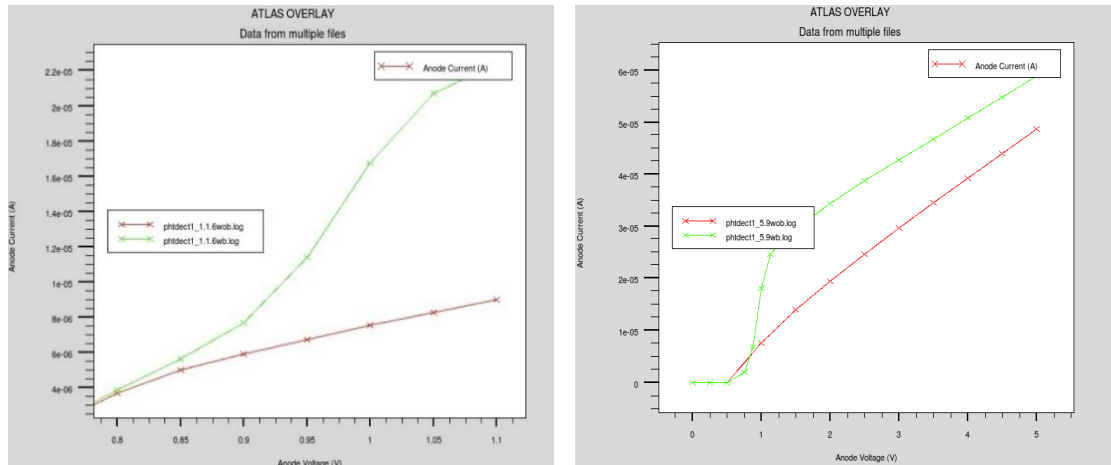


Fig. 5 Dark and Photo I-V Characteristics at different bias voltages.

4.3 Summary

This chapter discusses about a metal-semiconductor junction and its current-voltage characteristics of the proposed the Schottky diode. The advantages of schottky photodiodes like great quantum efficiency, small dark current with excessive UV/visible contrast. Furthermore, the Schottky type photodetectors can be of unlimited attention for the UV detection claims for their high rapidity and truncated noise performance. There is a strong market demand for uncooled photovoltaic (PV) detectors in mid-infrared (IR) wavelength range because cameras built with such detectors are much less expensive and more compact than cooled systems. CdS is a wide bandgap semiconductor material ($E_g \sim 2.4$ eV) with having ultrafast response and good stability for visible-light detectors.

Photodetector

Introduction

MSM Photodetector

Advantage of MSM Photodetector

Summary

5. Photodetector

5.1 Introduction

A photodetector is a device that transforms the light energy hooked on to some other custom of energy, such as thermal or electrical energy. The modern applications of photodetectors are numerous and they are important for fibre optics. Photography, astronomy, spectroscopy, plasma physics, high-energy physics. Sensors and monitoring [27].

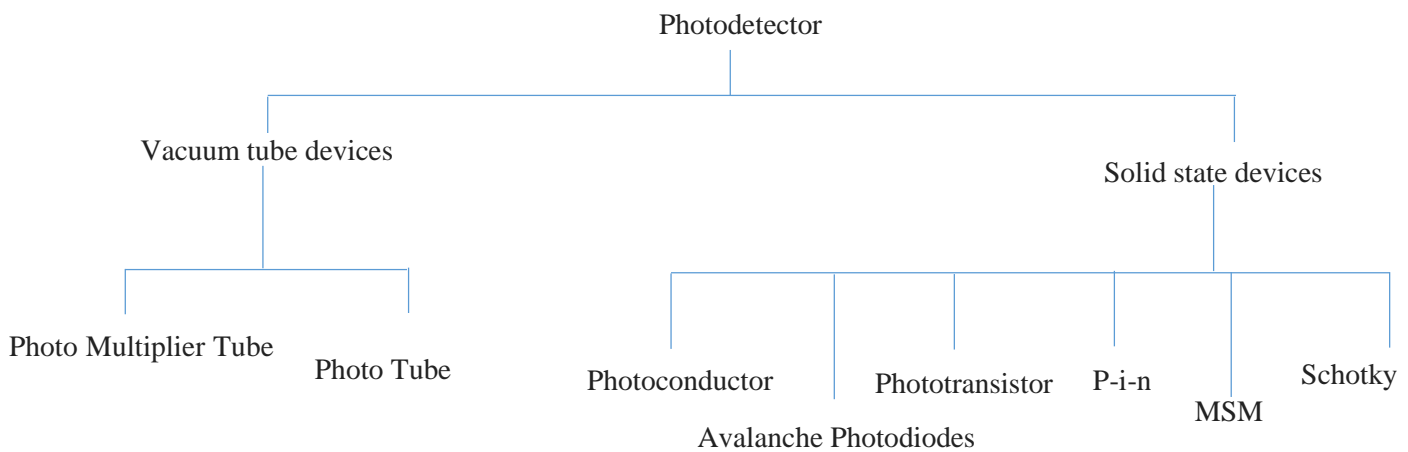


Fig.6 Classification of Photodetector.

A useful classification system for photodetectors is shown. While vacuum tube devices are still used, for example in ultra-sensitive photon-counting applications. Solid-state devices dominate the overall market. MSM photodetectors fall in the category of solid-state devices, without gain. These are the devices used for the highest speed applications.

5.2 MSM Photodetector

Metal-semiconductor-metal photodetectors are generally known as high-speed photodetectors and have valuable uses in the fields of communications, research and photograph. In brief, a metal-semiconductor-metal photodetector is a flat (planar) structure which has several layers. The "base" layer is a semiconductor layer which absorbs photons from a light source. Onto this layer are deposited metal electrodes. The electrodes are "interdigitated", or alternating, and form Schottky contacts. A Schottky contact is generically defined as a contact point between a metal and a semiconductor, which contact forms a barrier layer at the contact interface resulting in a rectifying current-voltage relationship. Generally, such contacts are extremely difficult to manufacture with a consistent barrier layer value [21].

Such photodetectors are known to be useful in optical communications systems, such as fibre-optic networks. Transmitted information is detected when incident light is absorbed by the semiconductor medium and the electron-hole pairs created are collected by the external circuit. For such a photodetector, coupling of the photodetector with the fibre optic light source is greatly simplified by the large area and thin nature of the MSM semiconductor. Further, due to their interdigitated nature, electron and hole "pairs" have only a small distance to travel before encountering a conductor, yielding a rapid response time.

MSM photodetectors naturally have a low capacitance per unit area, are easy to fabricate, and are especially suitable for use with field effect transistors. When manufactured in large size, they find application with fibre optic cables, enabling a better coarse alignment than before.

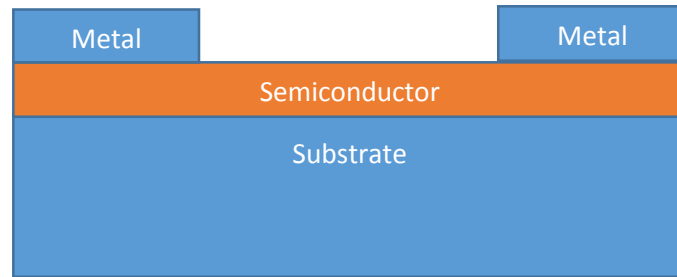


Fig.7 Schematic of MSM detector.

A conventional metal-semiconductor-metal photodetector is as illustrated in prior art FIG. 1. A semi-insulating base or substrate physically supports the structure and insulates the electrodes from each other and their surroundings. The active layer semiconductor is the area where photonic conversion to electrons and holes occurs and may be a separate layer or a portion of the semi insulating substrate. Metal electrodes are deposited onto the surface, and alternate between electrodes in an interdigitated manner [21].

5.2.1 Parameter related to photo detector

A photodetector's effectiveness is measured by its performance in many different parameters. These parameters include dark current, responsivity, speed, and spectral range. Dark current is generically defined as a current which flows in detectors when there is no radiant flux (light source) incident upon the electrodes. Or, in layman's terms, what is the current generated when there is total darkness. As an aside, this current may vary markedly between materials and temperatures.

Responsivity

Responsivity is the sensitivity of the photodetector, or a measure of how much incident light on the detector is collected and outputted as an external current. Conventional photodetectors are not very responsive, as the electrodes tend to shadow the "active" region of the semiconductor. It allows user to determine ahead of time how sensitive a

measuring circuit they will require to see the expected output or how much amplifier gain they need to get the signal levels up to a satisfactory level. Alternatively it tells how to determine the detected incident level from the output signal. The responsivity of a MSM phot detector is defined as:

$$R = \frac{I_{ph}}{P_{opt}} = \eta \frac{q\lambda}{hc}$$

Quantum efficiency

The quantum efficiency η ($0 \leq \eta \leq 1$) of a sensor is definite as the opportunity that a sole photon occurrence on the device engenders a photo-carrier duos that subsidizes towards the detector current. Once the several photons are incident, for instance practically in all situation, η is the ratio of the flux of produced electron-hole twosomes that provides to the photodetector current to the flux of incident photons. Altogether all incident photons cannot produce electron-hole duos as all incident photon never absorbed. Some photons may be reflected from the surface of the photodetector, or photo-generated pairs near the surface recombine due to the abundant recombination centres and fail to contribute to the current. The quantum efficiency can hence be inscribed as,

$$\eta = (1 - R) \zeta [1 - \exp(-\alpha d)]$$

Where R denotes the front surface reflectivity, α is the power absorption coefficient, d represents the wideness of the absorbing semiconductor coating, and ζ denotes the fraction of electron-hole couples that underwrite to the detector current [26].

Speed of the detector is also a primary consideration. Metal-semiconductor-metal photodetectors have an inherently high speed, as the interdigitated spacing of the electrodes leads to a very low capacitance per unit area. In other words, the speed

response is not limited by the resistance and capacitance product (RC time constant), but by the transit time of carriers from their creation point to the electrodes [21].

Last on the listed four physical qualities deemed most important is the spectral range of the response. As the range of electromagnetic radiation we call light extends from the infrared region (from 0.75 to 1000 microns in wavelength) to the ultraviolet (4000 angstroms to 400 angstroms), the more uniform the photodetector's response is over the spectral range, the better and the detector it is.

5.3 Advantages of MSM photo detector

MSM photodetectors are generally viewed as an alternative to p-i-n photodetectors for the highest-speed applications. In this section the main comparison points are briefly reviewed, and the advantages of the MSM photodetector are highlighted [27].

The main attributes of interest for a high-speed photodetector are its bandwidth, its responsivity, and its noise properties. The bandwidths of both p-i-n and MSM photodetectors are ultimately limited by carrier transit-times. For p-i-n detectors, the relevant carrier transit is across the intrinsic region of the device. In the MSM detector, it is the transit-time between adjacent fingers that is relevant. Without going into great detail, it can be stated that similar speeds are accessible for each type of detector [28], [29], [30]. In either case higher speeds are generally obtained at the expense of lower responsivity.

With regards to responsivity, p-i-n detection have a definite advantage. This is due to the partial shadowing of the absorption region by opaque metal fingers, in the top-illuminated MSM. The lower responsivity of the MSM is somewhat compensated by its lower inherent capacitance. In a typical optoelectronic receiver, a trans-impedance

amplifier follows the photodetector. The capacitance of the photodetector is important in determining the overall sensitivity of the receiver [31].

Three primary advantages can be identified for the MSM detector: fabrication and integration are simplified, the device is inherently symmetric, and the capacitance is lower. The p-i-n photodetector requires up to double as many processing steps. Additionally, several features of the p-i-n detector are further complex to realize in run-through: it is harder to grow heavily doped coatings precisely and repeatedly, ohmic electrodes require closely controlled recipes, and contacts essential to be made to dual coats of the epi-layer preparation. As a consequence, the p-i-n photodetector drives generally charge additional cost for fabrication.

5.4 Summary

This chapter starts with brief description different types of photodetector. An accumulative amount of consideration is being waged to assimilating high-speed photodetectors with microelectronic and photonic circuits' application. The metal-semiconductor-metal (MSM) alignment one of the favourable, having the benefit for its simple structure and high detection bandwidths up to hundreds of gigahertz, constructing them appropriate for high-speed on-chip optical connects [2], and optical communication systems [3]. Subsequent section followed by the parameters affecting the performance application of MSM detector and the application of over other photo diode.

Proposed MSM Photodetector

Introduction

Proposed Structure

Results and Discussions

6. Proposed MSM Photo detector

6.1 Introduction

Cadmium Sulphide (CdS) belonging to the II-VI direct bandgap compound semiconductor group is widely known as an n-type window material for optoelectronic devices [11-14]. CdS is a wide bandgap semiconductor material ($E_g = 2.4$ eV) with having ultrafast response and good stability for visible-light detectors. As for photo detection CdS is integrating with a different inferior bandgap semiconductor in suitable arrangement of energy levels, broaden the response spectra to longer wavelength forthcoming headed for adjacent to infrared range. The metal-semiconductor-metal (MSM) alignment one of the favourable, having the benefit for its simple structure and high detection bandwidths be reach up to gigahertz ranges, constructing them appropriate for very fast on-chip optical connects [2], and optical communication systems [3].

6.1 Proposed Structure

The MSM detector is a two terminal device consisting of schottky diode connected back to back. The schematic diagram of proposed MSM Photodetector is shown in Figure 1. The photodetector was fabricated with thickness (h) of $3.5\text{ }\mu\text{m}$ of n-type material epitaxial grown CdS coating having $3 \times 10^{15}/\text{cm}^3$ of doping concentration followed by about $400\text{ }\mu\text{m}$ thickness of n+ CdS substrate with $5 \times 10^{18}/\text{cm}^3$ doping concentration. Schottky contacts have made by using a thickness of 200 nm of Tungsten (W) as electrode. Because of its anti-reflection and tall transmittance property a 200nm thick

ZnSe that can absorb a wavelength of range 0.6 μm to 16 μm is used between the electrodes. The energy band diagram of a MSM photodetector under electric bias is shown in Figure 2. Figure 9 and 10 shows the simulated structure using ATLAS under dark condition and illumination of light of wave length of 8 μm .

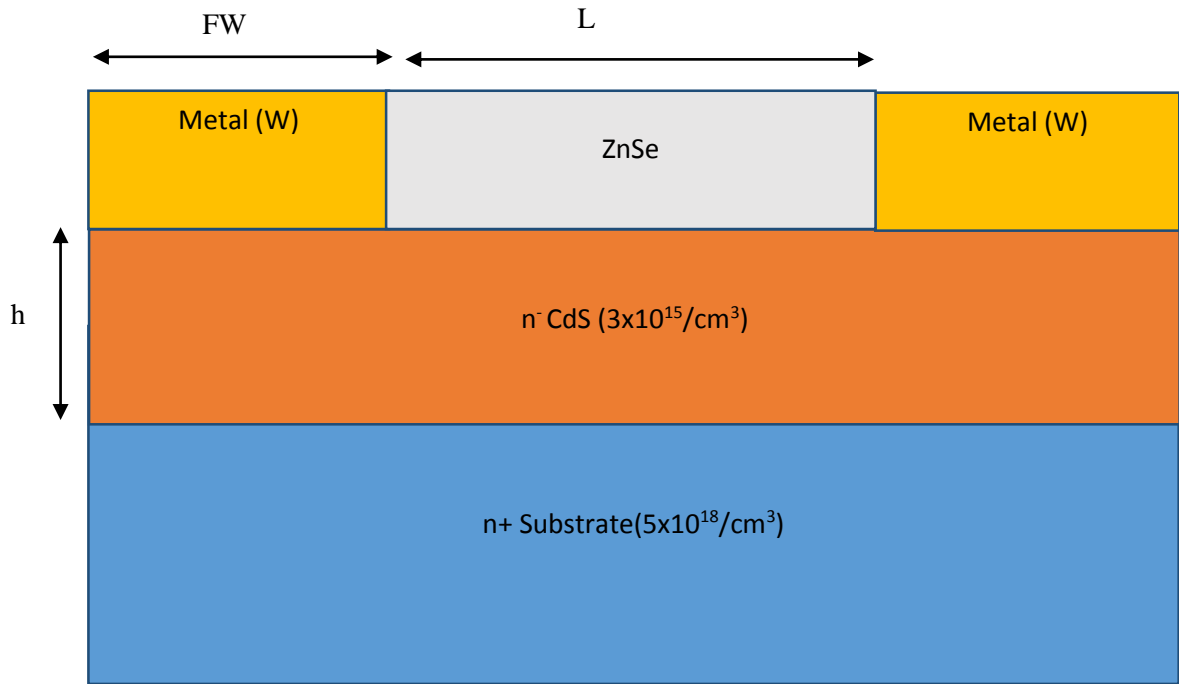


Fig.8 Schematic of Proposed MSM Photodetector.

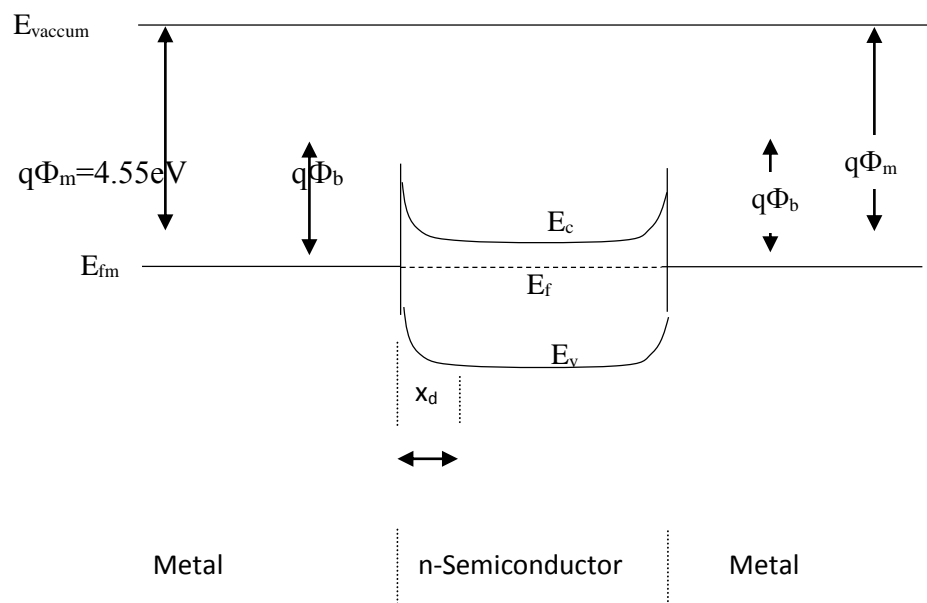


Fig.9 Energy band diagram of MSM Photodetector.

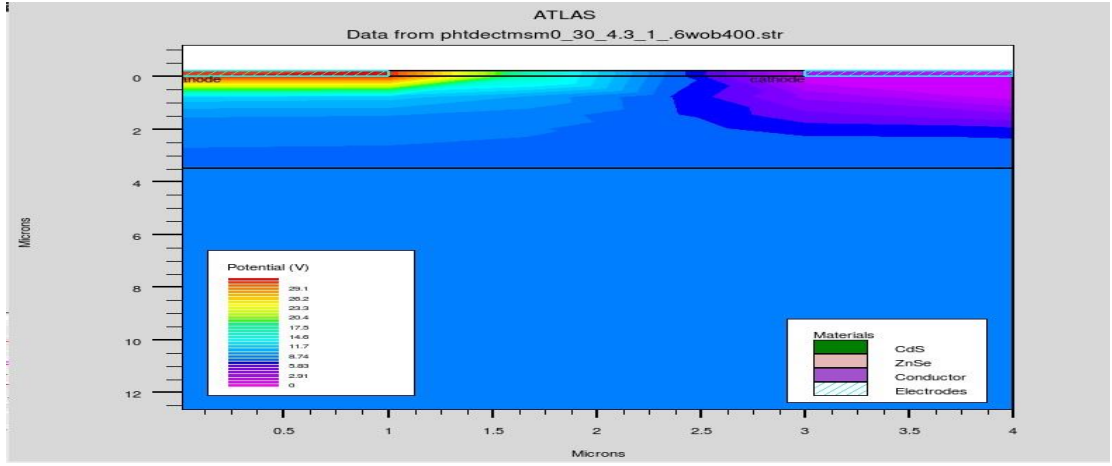


Fig.10 Proposed Structure under dark condition.

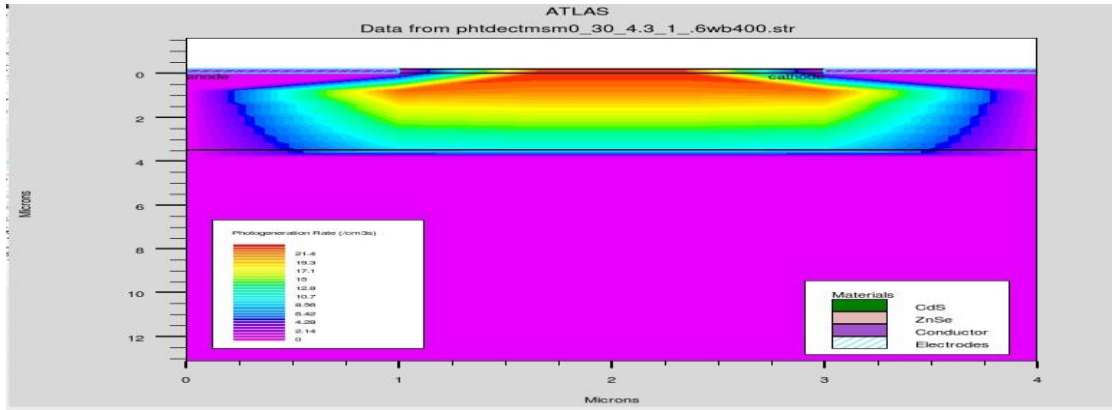


Fig.11 Structure of MSM photodetector under illumination of light of wavelength 8 μ m.

6.3 Results and discussion

For proposed MSM photo detector, the dark current is measured as 4×10^{-9} A with the photo current has been found out two order higher i.e. 1.03×10^{-7} A at 16 V DC bias. The responsivity can be defined as

$$R = \frac{I_{ph}}{P_{opt}} = \eta \frac{q\lambda}{hc}$$

Where I_{ph} represents the illuminated current of the detector by absorption of incident light, P_{opt} denotes the incident optical power at given wavelength λ , η represents

quantum efficiency, h is the Planck constant and c is the speed of light [32]. The spectral response of the detector at various wavelengths is shown in Figure 3 and the peak responsivity of the detector has been found out 2.96 A/W at wavelength 8 μm . So to get the optimum response all the simulation has been done at 8 μm wavelength for the proposed structure.

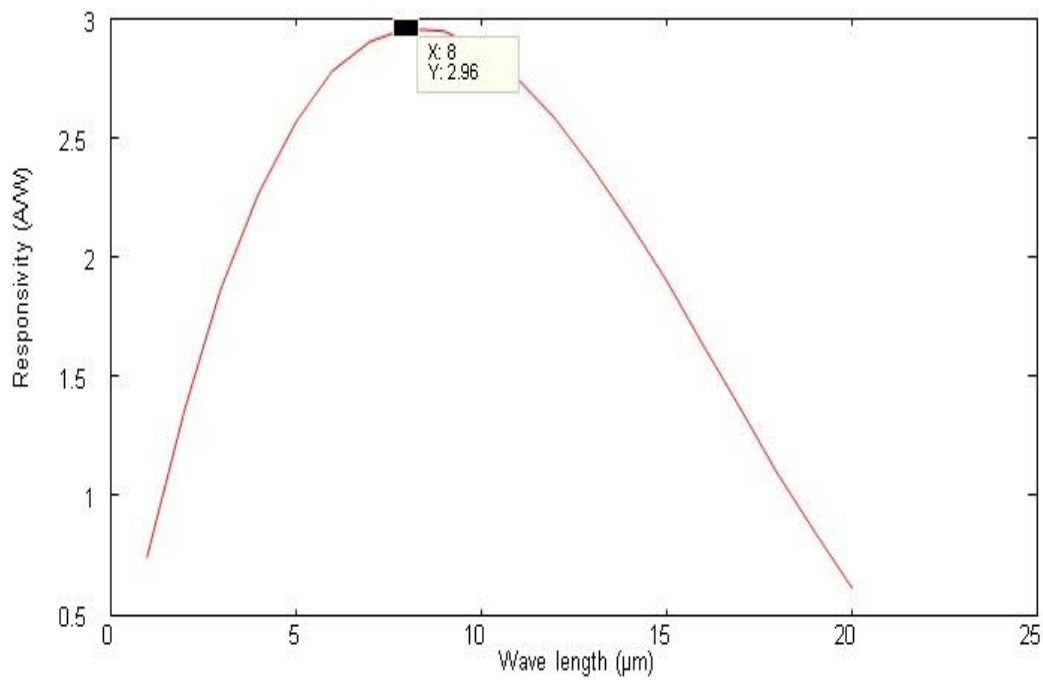


Fig.12 Responsivity at various wavelength.

The dark and photo current-voltage characteristics are a significant factor for a photodetector that are simulated and shown in Figure 4 and 5 respectively with different bias voltages at a number of finger widths (FW). Two kinds of detector topology have validated with finger spacing (L) 2 and 5 μm among the metal electrodes. It has been set up that the dark current is increasing with the intensification in applied electrical energy with realizing that dark current is accumulative with the increase in finger widths [24, 25]. We have found that at 10V DC bias the dark current is 1.28×10^{-9} A at

1 μm finger width while it is up to $2.26 \times 10^{-8} \text{ A}$ when the finger width is 10 μm . There is not considerable difference in dark currents for 2 and 5 μm spacing. It has been observed that photocurrent is increasing with the increase in finger width due to large illuminated area.

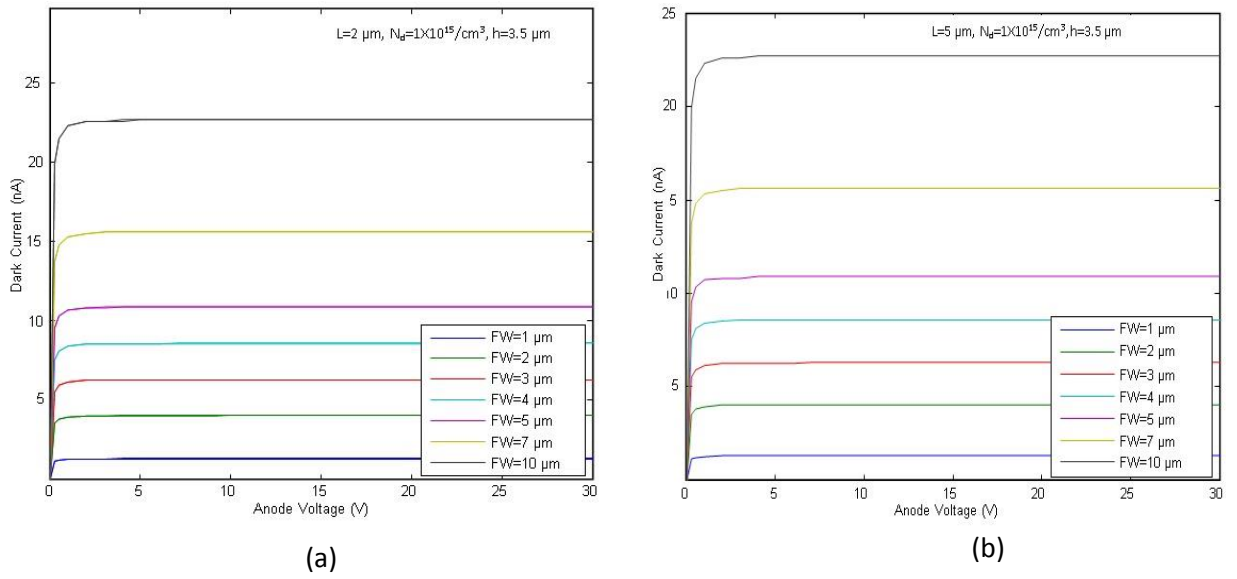


Fig.13 Dark current-voltage characteristics of proposed MSM with different finger widths for finger spacing (a) 2 μm (b) 5 μm .

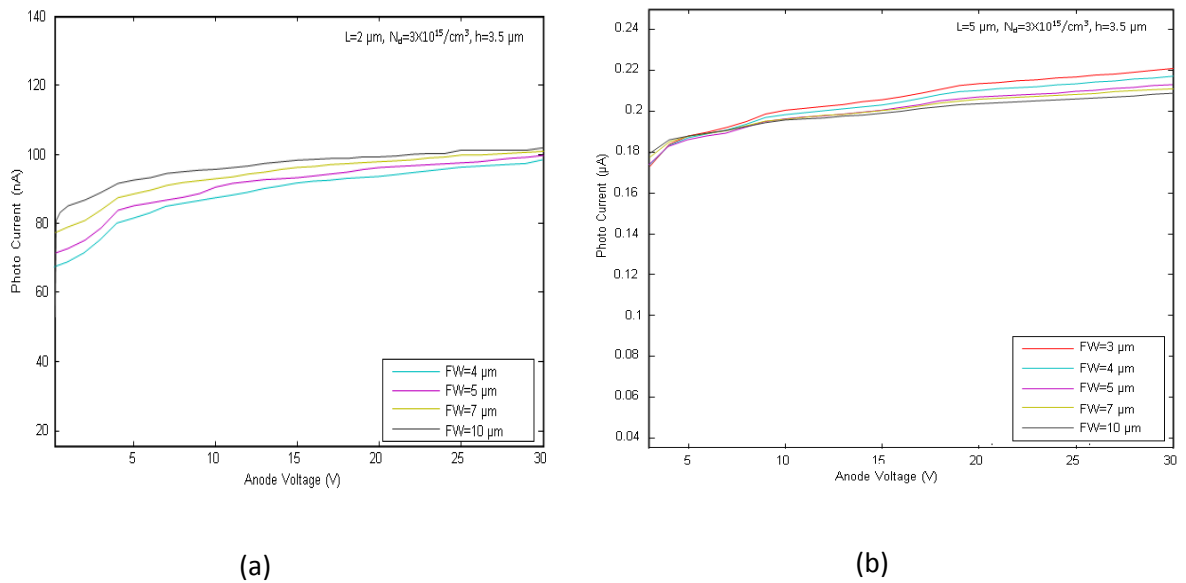


Fig.14 Illuminated current-voltage characteristics of proposed MSM per different finger widths at finger spacing (a) 2 μm (b) 5 μm .

Figure 6 illustrates the dark current-voltage characteristics for the projected MSM photo-detector at different spacing between the electrodes. It can be observed that these device shows almost same dark current 10^{-9} A for different finger spacing. It also proposes that dark current with 5 μm spacing is more to that of the detector with 2 μm .

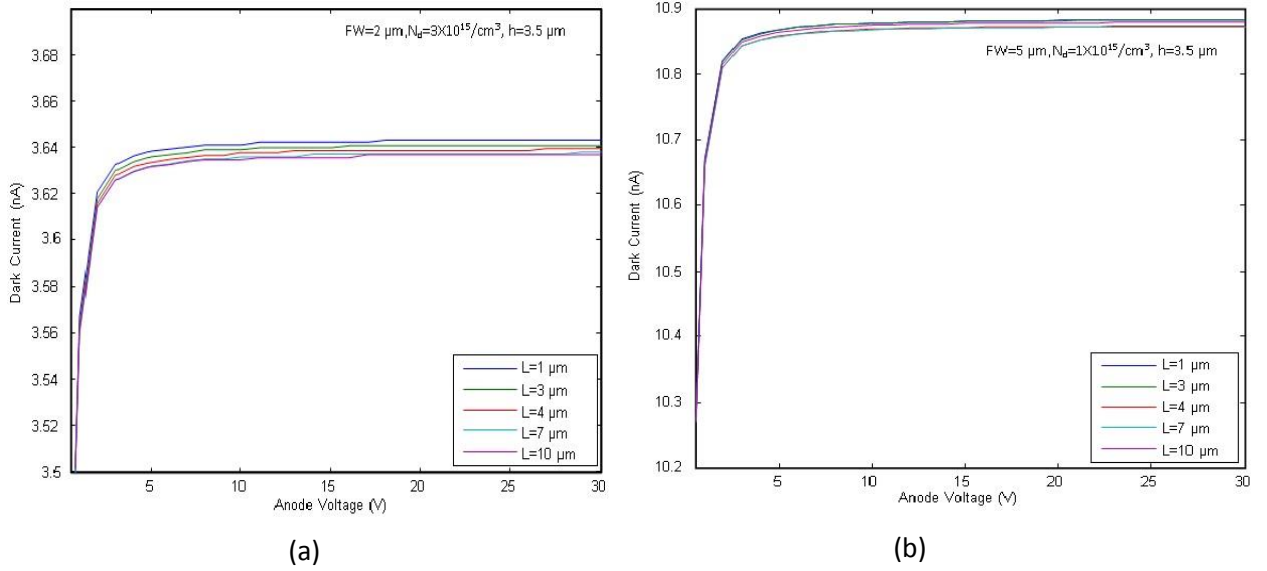


Fig.15 Dark current-voltage characteristics of proposed MSM with changed finger spacings at finger width (a) 2 μm (b) 5 μm .

Figure 7 displays the variation of photocurrent with changed finger spacing. It has been brought into being that photocurrent is changed more considerably as compared to dark current with various finger spacing. Also, it shows that photocurrent rises with the escalation in finger spacing that indicates the dependence of photo generation rate on the active area. This is consistent with previous results reported by others [24].

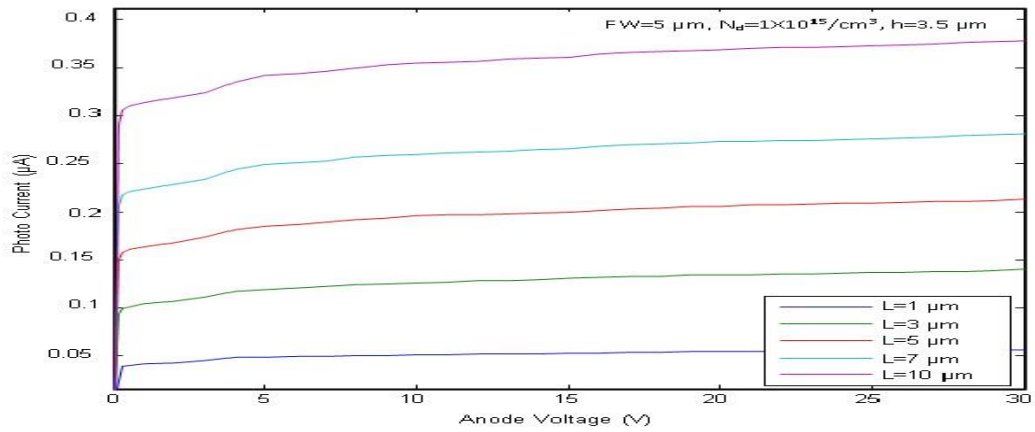


Fig.16 Photo current-voltage characteristics of proposed MSM Photo-detector with altered spacing.

Figure 8 showing the current-voltage characteristics of the proposed photodetector at dissimilar epitaxial layer concentration. Here we kept the finger width, finger spacing and thickness epitaxial layer 2, 5 and 2 μm respectively. It can be observed from the graph that the dark current increases whereas the photocurrent reduces with the rise in epitaxial layer concentration that verifies that the lesser the contextual level, the superior is the illuminated current.

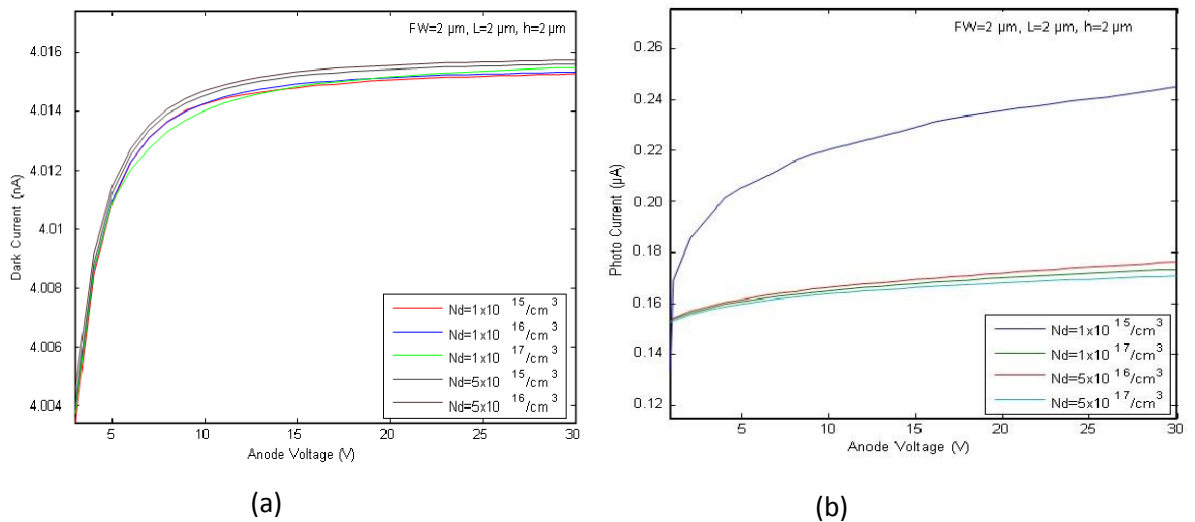


Fig.17 current-voltage characteristics of proposed with changed epitaxial carrier concentration.(a)Dark I-V characteristics (b) Illuminated I-V characteristics.

The consequence of epitaxial layer width on the current-voltage characteristics has been shown in Figure 9 and 10 for the finger spacing and width kept at 5 and 2 μm respectively. It has been found out that dark current reduces with rise in thickness of the epitaxial film with a less variation whereas the photocurrent increases with the intensification in width of the epitaxial coating. So by choosing the adequate thickness we can enhance the performance of the MSM photodetector. Epitaxial layer have not to be too dense or tinny as excessively active level not only require lengthy growth time period but also disturbs the transient response of the detector. Also, the thin epitaxial layer may reduce its photo response due to insufficient photo absorption.

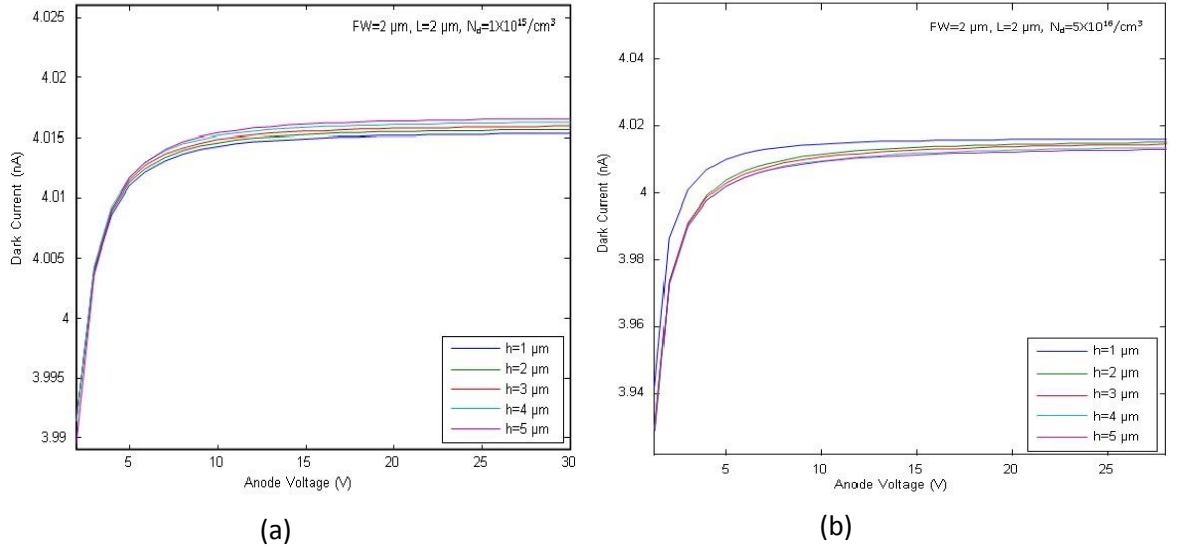
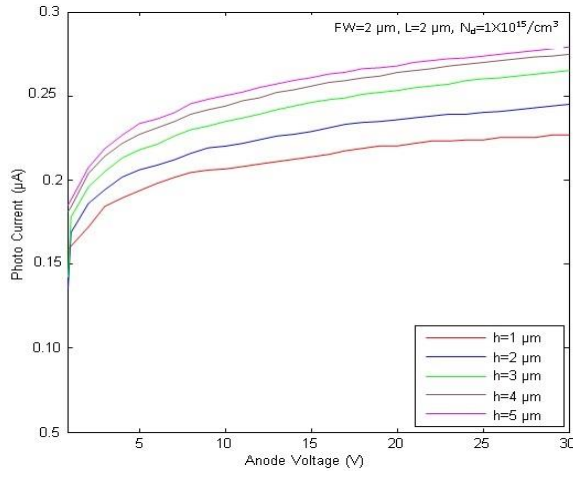
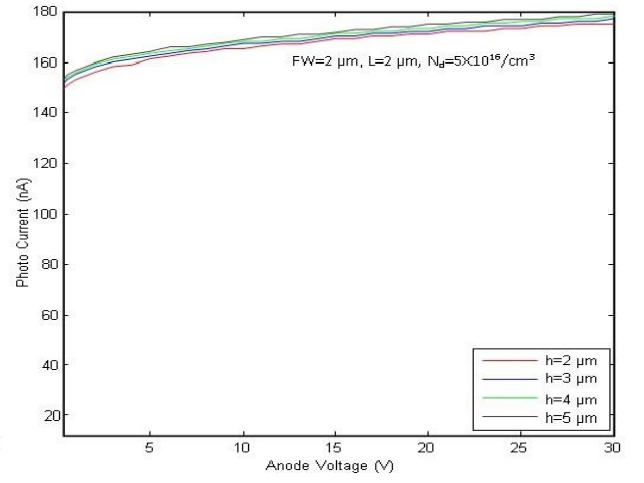


Fig.18 Dark current-voltage characteristics of proposed photo-detector per epitaxial layer widths. (a) $N_d = 1 \times 10^{15} / \text{cm}^3$ (b) $N_d = 5 \times 10^{16} / \text{cm}^3$.



(a)



(b)

Fig.19 Photo current-voltage characteristics of proposed per epitaxial layer widths.

(a) $N_d=1 \times 10^{15}/\text{cm}^3$ (b) $N_d=5 \times 10^{16}/\text{cm}^3$.

7. Conclusion

7.1 Outcome of the Work

The objectives of this effort were basically threefold: to improve the technology of basic MSM photodetectors: Inspect methods to improve their responsivity, and develop techniques of mixing several MSM photodetectors in a broadband array. The work was accompanied with precise applications in thoughts. In particular broadband optoelectronic switching and signal processing systems. The current-voltage (I-V) characteristics of the proposed MSM photodetector are simulated using Silvaco ATLAS, considering different parameters for optimising their performance. The result shows that the effect of finger width of photodetector is more significant on the dark current whereas the effect of finger spacing is for the photocurrent. The effect of epitaxial layer concentration is studied where finding shows that the dark current increases whereas the photocurrent reduces with the rise in epitaxial layer concentration that verifies that the lesser the contextual level, the superior is the illuminated current. The photocurrent also increases with the increase in thickness of the epitaxial layer. So by choosing the adequate thickness we can enhance the performance of the MSM photodetector. This results will helpful while designing MSM photodetector to optimise their performance.

7.2 Future Scope

We had simulated our structure using ATLAS Silvaco and studied the current-voltage characteristics. Modelling of our proposed structure can also be done and result can be validated with our simulated result.

References

- [1] A. Rogalski, “Heterostructure Infrared Photodiodes”, *Semiconductor Physics Quantum Electronics & Optoelectronics*, vol.3, pp.111-120, 2000.
- [2] S. Assefa, F. Xia, and Y. A. Vlasov, “Reinventing germanium avalanche photodetector for Nan photonic on-chip optical interconnects”, *Nature*, vol.464, pp. 80–84, 2010.
- [3] M. Y. Liu and S. Y. Chou, “Internal emission metal-semiconductor- metal photodetectors on Si and GaAs for 1.3 μm detection”, *Appl. Phys. Lett.*, vol. 66, pp. 2673–2675, 1995.
- [4] H. H. Chen, Y. C. Su, W.-L. Huang, C. Y. Kuo, W. C. Tian, M. J. Chen, and S. C. Lee, “A plasmonic infrared photodetector with narrow bandwidth absorption”, *Appl. Phys. Lett.*, vol. 105, pp. 023109, 2014.
- [5] P. Fan, U. K. Chettiar, L. Cao, F. Afshinmanesh, N. Engheta, and M. L. Brongersma, “An invisible metal–semiconductor photodetector”, *Nat. Photonics*, vol. 6, pp. 380–385, 2012.
- [6] L. Cao, J. S. Park, P. Fan, B. Clemens, and M. L. Brongersma, “Resonant germanium Nano antenna photodetectors”, *Nano Lett.*, vol. 10, pp. 1229–1233, 2010.
- [7] S. Collin, F. Pardo, R. Teissier, and J. L. Pelouard, “Efficient light absorption in metal–semiconductor–metal nanostructures”, *Appl. Phys. Lett.*, vol. 85, pp. 194–196, 2004.
- [8] G. Konstantatos and E. H. Sargent, “Solution-processed quantum dot photodetectors”, *Proc. IEEE*, vol. 97, pp. 1666–1683, 2009.

- [9] G. Konstantatos, I. Howard, A. Fischer, S. Hoogland, J. Clifford, E. Klem, L. Levina, and E. H. Sargent, “Ultrasensitive solution cast quantum dot photodetectors”, *Nature*, vol. 442, pp. 180–183 2006.
- [10] R.P. Chang and D.C. Perng, “Near-infrared photodetector with $\text{CuIn}_{1-x}\text{Al}_x\text{Se}_2$ thin film”, *Appl. Phys. Lett.*, vol. 99, pp. 081103, 2011.
- [11] D. Patidar, R. Sharma, N. Jain, T. P. Sharma and N. S. Saxena, “Optical properties of CdS sintered film”, *Bull. Mater. Sci.*, vol. 29, pp. 21–24, 2006.
- [12] C. S. Ferekides, D. Marinskiy, V. Viswanathan, B. Tetali, V. Palekis, P. Selvaraj, and D. L. Morel, “High efficiency CSS CdTe solar cells”, *Thin Solid Films*, vol. 361, pp. 520–526, 2000.
- [13] K. Orgassa, U. Rau, Q. Nguyen, H. W. Schock, and J. H. Werner, “Increase in short-wavelength response of encapsulated CIGS devices by doping the encapsulation layer with luminescent material”, *Prog. Photovoltaics*, vol. 10, pp. 457–463, 2002.
- [14] N. Sfina, N. Zeiri, A. B. Nasrallah, and M. Said, “CdS/PbSe heterojunction for high temperature mid-infrared application”, *Mater. Sci. Semicond. Process*, vol. 19, pp. 83–88, 2014.
- [15] Atlas user’s manual. (2008). Device Simulation Software, Silvaco International, Santa Clara, CA.
- [16] Zehor Allam¹, Abdelkader Hamdoune, Chahrazed Boudaoud, “ The electrical properties of InGaN/GaN/AlN MSM photodetector with Au contact electrodes”, *Journal of Electron Devices*, Vol.17, pp.1476-1485, 2013.
- [17] D Patidar, R Sharma, N Jain, T P Sharma and N S Saxena*, “Optical properties of CdS sintered film”, *Bull. Mater. Sci.*, Vol. 29 No 1, pp. 21–24, 2006.

- [18] T. Munir , A. Abdul Aziz, M. J. Abdullah, N. M. Ahmed , A. Y. Hudeish, “Optimum n-GaN Schottky diode current-voltage Characteristics by using different metal contact”, Solid State Science and Technology, Vol. 14, No. 1 pp.147-152, 2006.
- [19] N. Sfina, N. Zeiri, A. B. Nasrallah, and M. Said, “CdS/PbSe heterojunction for high temperature mid-infrared application”, Mater. Sci. Semicond. Process, vol. 19, pp. 83–88, 2014.
- [20] Ito, M. (1988).”U.S.Patent No. 4,763,176”.Washington, DC: U.S.Patent and Trademark office.
- [21] Paul R. Berger, P.R., Del, N., Gao, W., Mass, W.” U.S.Patent No. 5,777,390”. Washington, DC: U.S.Patent and Trademark office.
- [22] Yanbin An, Ashkan Behnam, Eric Pop, and Ant Ural,” Metal semiconductor-metal photodetectors based on graphene/p-type silicon Schottky junctions”, Applied Physics Letters, Vol.102 No.1, pp. (013110)1-5, 2013.
- [23] C. K. Wang, S. J. Chang, Y. K. Su, Y. Z. Chiou, S. C. Chen, C. S. Chang, T. K. Lin, H. L. Liu, and J. J. Tang,” GaN MSM UV Photodetectors With Titanium Tungsten Transparent Electrodes”, IEEE Transactions On Electron Devices, VOL. 53, NO. 1, pp.38-42, 2006.
- [24] J. Zhang, Y. Yang, L. Lou, and Y. Zhao, “Current-voltage characteristics simulation and analysis of 4H-SiC metal-semiconductor-metal ultraviolet photodetectors”, Chinese Optics Letters, vol. 6, pp.615-618, 2008.
- [25] C. Bin., Y. Yintang, L. Yuejin, and L. Hongxia, “Simulation and optimization of a 6H-SiC metal–semiconductor–metal ultraviolet photodetector”, Journal of Semiconductors, vol. 31, pp. (064010)1-6 2010.

- [26] Tut, T. (2008). *GaN/AlGaIn-based uv photodetectors with performances exceeding the pmts*. Ph.D. Thesis. Reading University: China
- [27] DeCorby, R.G.(1998). *Optimization of Metal-Semiconductor-Metal Photodetectors and Advanced Photodetector Structures*. Ph.D. Thesis. Reading University: Canada.
- [28] L. Figueroa, C.W. Slayman. "A novel heterostructure interdigital photodetector (HIP) with picosecond optical response". IEEE Electronic Device Letters, vol. EDL-2, no. 8, pp. 208-210, 1981.
- [29] J.E. Bowers, "Ultra wide-band long-wavelength p-i-n photodetectors", Journal of Light wave Technology. Vol. LT-5. No. 10, pp. 1339-1350, 1987.
- [30] E.H.Bottcher,D.Kuhl,F.Heironymy,E.Droge,T.Wolf,D.Bimberg,"Ultrafast semi insulating InP:Fe-InGaAs:Fe-InP:Fe MSM photodetectors: modelling and performance",IEEE Journal of Quantum Electronics,Vol.28,no.10.pp,2343-2357,1992.
- [31] E.John, M.Das,"Design and performance analysis of InP-based high speed and high sensitivity optoelectronic integrated receivers", IEEE Transactions on Electron Devices, Vol.41.no.2.pp.162-171, 1994
- [32] P. Hazra, S. K. Singh, and S. Jit, "Ultraviolet Photo detection Properties of ZnO/Si Heterojunction Diodes Fabricated by ALD Technique Without Using a Buffer Layer", Journal of Semiconductor technology and science, vol.14, pp.117-123 , 2014.